Dispersive Raman Spectroscopy for the Nondestructive and Rapid Assessment of the Quality of Southern Italian Honey Types

JOURNAL OF LIGHTWAVE TECHNOLOGY, VOL. 34, NO. 19, OCTOBER 2016

Dispersive Raman Spectroscopy for the Nondestructive and Rapid Assessment of the Quality of Southern Italian Honey Types

Anna Grazia Mignani, *Member, IEEE*, Leonardo Ciaccheri, Andrea Azelio Mencaglia, Rosa Di Sanzo, Sonia Carabetta, and Mariateresa Russo

Abstract

Raman spectroscopy performed using optical fibers, with excitation at 1064 nm and a dispersive detection scheme, was utilized to measure a selection of unifloral honeys produced in the Italian region of Calabria. The honey samples had three different botanical origins: chestnut, citrus, and acacia. A multivariate processing of the spectroscopic data enabled us to distinguish their botanical origin, and to build predictive models for quantifying important nutraceutic indicators, such as the main sugars and potassium. Furthermore, the Raman spectra of chestnut honeys were compared with the taste profile measured by an electronic tongue: A good correlation to a bitter-savory taste was obtained.

This experiment indicates the excellent potential of Raman spectroscopy as a modern analytical tool for the nondestructive and rapid multi-component analysis of food quality indicators.

Index Terms—Food products, labeling, pattern analysis, predictive models, Raman scattering, sugar.

I. INTRODUCTION

One of the major needs of honey producers and retailers is to have effective devices available for the nondestructive and rapid assessment of honey quality types, above all their botanical origin and nutraceutic profile. In fact, the most demanding consumers tend to choose unifloral honeys, that is, ones made from the pollens of the same type of flower, and are also looking for information of about the sugar profile and the concentration of potassium. Indeed, the typical and unique taste of a unifloral honey, as well as its nutraceutic properties, are important indicators that strongly influence the preferences of consumers who are willing to buy high-end products.

Actually, no honey is purely unifloral: in fact, the term *unifloral* is used to describe honey in which most of the nectar comes from a single plant type. Microscopy for pollen analyses, organoleptic assessment, and other physico-chemical analyses are currently used for botanical authentication [1], [2]. These techniques have been discussed within the International Honey Commission of Apimondia, and have been recognized as being valid for authentication purposes [3]. The said types of analyses can be carried out only by trained personnel in costly analytical laboratories, and have the main disadvantage of being destructive and time-consuming. Hence, new technologies are envisaged for assessing the botanical origin of honey quickly and at low cost.

Optical spectroscopy is currently emerging as a modern and *green* analytical technique for intact food analyses [4]–[6]. In fact, the nondestructive nature of light measurements enables no-contact and rapid checks, in addition to multi-component analysis, without product damage and/or waste. Moreover, the use of reagents or chemical treatments is not necessary, meaning that the problem of waste disposal is thus avoided. Optical techniques, which are frequently used in combination with a chemometric processing of spectroscopic data [7], [8], have been tested for years also for analyzing honeys. Near infrared spectroscopy has been extensively experimented for confirming their botanical origin, as well as for fraud detection, for geographical classification, and for predicting the content of antioxidants [9]–[19]. Similar results for authentication have been obtained by means of colorimetry [20] and fluorescence spectroscopy [21]–[27].

Raman spectroscopy has also been successfully experimented for rapid quality checks. While absorption and fluorescence spectra show broad peaks that result from the convolution of the many

overlapping bands, which are insufficiently resolved for the purposes of multi-component analysis, Raman spectroscopy shows clear-cut bands that identify the molecular composition and can therefore provide a better quality assessment.

The Raman experiments presented up to now for honey analysis have made use of compact devices with excitation at 785 nm and dispersive detection schemes [28]–[30], or else of more cumbersome devices with excitation at 1064 nm and the use of Fourier transform detection devices [31]–[34]. Both setups have certain disadvantages. The excitation at 785 nm causes a natural fluorescence; consequently, a subtraction of the fluorescence offset is needed, thus risking that some relevant spectroscopic information be ignored.

The fluorescence effect is greatly mitigated by using excitation at 1064 nm; however, the Fourier transform detection scheme is cumbersome, and is not suitable for use in a portable device.

The objective of this paper was to use an innovative setup for Raman spectroscopy, with excitation at 1064 nm and a compact dispersive detection scheme, combined to multivariate processing of the spectroscopic data, in order to assess the quality of honeys produced in the Calabrian region, which is in southern Italy. This experimental setup makes use of optical fibers, which provides stability of the light signals, compactness, and ease in the alignment.

This device and a similar data processing have been recently experimented by the same authors for characterizing artificial sweeteners [35].

The honey samples considered had three different botanical origins: chestnut, citrus, and acacia.Amultivariate processing of the spectroscopic data enabled us to distinguish their botanical origin, and to build predictive models for quantifying important nutraceutic indicators, such as the main sugars and potassium.

Furthermore, the Raman spectra of chestnut honeys were compared with the taste profile measured by an electronic tongue, and a good correlation to a bitter-savory taste was obtained.

These results, indicating the excellent potential of Raman spectroscopy as an analytical tool for the nondestructive and rapid assessment of food quality, complement the findings previously presented in an earlier paper by the same authors [36].

The innovation suggested by this paper is the possibility of measuring many quality indicators of the honey during the production, which is of particular interest for industrial applications in product quality control. In addition, a nutraceutic labelling at the time of packaging can be achieved, which is considered a new marketing action particularly attractive for consumers.

II. HONEYS ANALYZED

A set of 13 unifloral honeys was considered, as summarized in Table I. These were collected in different areas of Calabria, which has rich vegetation and a pristine habitat—ideal conditions for the production of excellent honey. These samples had three different botanical origins: chestnut, citrus, and acacia, and were produced in different geographical areas, both in the mountains and near the coast.

The chestnut honeys had a characteristic herbal, slightly tannic aroma and taste, with a dark yellowish-brown color and amber hues. The citrus honeys had a mixed taste of orange, maltose, other di-saccharises, and tri-saccharides (lower plot).

lemon, mandarin, and bergamot, and were characterized by a light amber color. The acacia honeys had a fruity, delicate and sweet taste, with a very transparent lemonish tallow-green color.

Conventional analytical techniques based on destructive laboratory procedures were used to measure the most important nutraceutic indicators in order to obtain precise reference data for correlation to Raman spectra. The sugar profile, i.e., the concentration of main sugars (glucose and fructose) and of the whole content of di- and tri-saccharides, in addition to potassium (the most abundant mineral in honey) were considered to be nutraceutic indicators. Indeed, these quality indicators are of interest for both dietetic and production issues.

High-performance anion-exchange chromatography with pulsed amperometric detection was used to measure the sugar profile [37]. The boxplots of Fig. 1 show the results of these measurements. The

upper figure depicts the spread of concentration for glucose and fructose. The lower figure shows the concentration spread of maltose, other di-saccharides (trehalose, isomaltose, koijbiose, nigerose, summarized as DS-TIKN), and tri-saccharides (isomaltotriose, erlose, panose, summarized as Total TS).
Inductively coupled plasma emission spectroscopy [38] was used to measure the concentration of potassium, which was found to be in the 0–6 μg/g range.

III. RAMAN SPECTROSCOPY SETUP

The Raman effect occurs when monochromatic light interacts with a molecule and exchanges energy with its electron cloud.
In addition to the light scattered with an unchanged wavelength (elastic or Rayleigh scattering), a small fraction of the order of 10–6 of the incident light is scattered inelastically, and the wavelength shift depends on the variation of the vibrational state of the molecule. This wavelength shift does not depend on the illumination wavelength, but only on the molecular vibrational levels. Hence, since it is a unique expression of the molecular structure, the Raman spectrum is considered to resemble a molecular fingerprint—it literally serves as a signature [39].
The novel instrument for the Raman spectroscopy used in this experiment provided laser excitation at 1064 nm, which is not
the most popular wavelength for Raman experiments, since the Raman signal is inversely proportional to the fourth power of the laser wavelength. However, this long excitation wavelength makes it possible to avoid fluorescence effects that are common in honeys and might mask the weak Raman signal. The detection unitwas based on a dispersive scheme that provided a more compact unit with respect to the Fourier transform configurations frequently used in other Raman instruments. Three spectrometers made it possible to operate over a wide wavenumber range (300–3200 cm–1), and a thermoelectrically-cooled InGaAs array that was set at –55 °C served as detector. A resolution of 4 cm–1 was obtained [40].
Fig. 2 shows a diagram of the Raman spectroscopy instrument, which made use of two optical fibers. One was for bringing the laser light to a microoptic unit, and the other served to guide the backscattered Raman signal back to the entrance slit of the spectrometer. A detailed view of the optics inside the Raman probe is shown in Fig. 3. The laser power is 400 mW (MiniLite-1064, BaySpec, CA, USA); its light is delivered to the Raman probe via a 105 μm optical fiber, and then collimated by a lens. The laser line is cleaned by a narrow band-pass 1064 nm laser clean-up filter (Semrock, NY, USA). After passing a dichroic beamsplitter (Semrock, NY, USA), the light is focused by a lens (f = 6 mm) onto the sample, and the same lens is used to collected the back-scattered light. Raman signals whose wavelengths are longer than 1064 nm are reflected by the dichroic beamsplitter, and further cleaned by a long-pass filter, before being coupled into a 200 μm optical filter and sent back to the spectrometer. The samples were analyzed inside a 4-mL vial. This vial was inserted in a suitable holder that was butt-coupled to the microoptic unit. The entire instrument was interfaced with a laptop PC that included software for the management of hardware options (laser power, integration time, wavenumber range, etc.), and for the acquisition, display, and first processing of spectra.

IV. RAMAN SPECTRA OF HONEYS

The measured Raman spectra of the honey samples are shown in Fig. 4: each spectrum is the average of the spectra of each botanical origin. They are displayed in the most informative spectroscopic range for honey, namely 700–1700 cm–1. The integration time was 20 s, and an average of three scans was considered for every sample. In order to reduce any possible uncertainties caused by source intensity fluctuations, the spectra were normalized to the intensity at 630 cm–1. This wavenumber corresponds to the Raman peak with the highest intensity among all the fructose peaks. This kind of normalization, which was previously suggested in the literature [see Reference 32], is justified because fructose concentration has a small variation within our dataset (its standard deviation is barely 4% of its mean value), and is therefore not a good discriminating variable. On the other hand, the peak at 630 cm–1

is relatively free of interference from other sugars. Therefore, fixing its amplitude alters the spectral contributions of other sugars very little. Note that pure fructose peaks at 821, 867 and 1267 cm–1 show very low variance because of the normalization. Instead, high variance is shown where other sugars contribute, in different proportions, to the Raman spectrum: see, for example, the bands at 1070 and 1127 cm–1, the "valley" at 840 cm–1 and the background above 1550 cm–1.
Indeed, the Raman spectra of honeys are an expression of the different sugar composition common to the different honeys 41]. A better understanding of the contribution of the various sugars to the Raman spectra can be obtained by considering water solutions of glucose, fructose, maltose, and sucrose. Fig. 5 shows the Raman spectra of water solutions with a 30% w/w concentration of these sugars. As for the spectra of the honeys, the average of three measurements was considered. The spectra of these four sugar types were normalized to the height of the corresponding main peak. They occurred at 630 cm–1 for fructose, 520 cm–1 for glucose, and 548 cm–1 for sucrose and maltose. Table II summarizes the most important wavenumbers relative to these main sugars, which characterize the Raman spectra of honeys.

V. DISTINGUISHING THE BOTANICAL ORIGIN

The Raman spectra were processed using Principal Component Analysis (PCA), which is one of the most popular methods for data dimensionality reduction and explorative analysis [42]. PCA projects the entire set of spectra onto a lower dimension subspace, while retaining the maximum fraction of data variance among all orthogonal subspaces with the same dimension. In practice, PCA makes a linear transformation that converts the original measured variables into new orthogonal variables called Principal Components (PC). The first Principal Component (PC1), has the largest possible variance among all possible linear combinations of the starting variables; the second Principal Component (PC2) has the maximum of the residual variance, and so on. The values that represent the samples in the new space are called scores, while the coefficients that express the PCs as functions of the old variables are called loadings [43].
For purposes of classification, two PCs (PC1 and PC2) were then selected, and a matrix of 13 rows (samples) × 2 columns (PCs) was created. This matrix was processed by means of Linear Discriminant Analysis (LDA), which is a robust and reliable technique for automatic object classification [44]. Both PCA and LDA processing were carried out by a custom MATLAB code. A grid of 81 × 201 points was generated and classified in the LDA space. Then, a contour plot of their "class" value was superimposed to the score plot in order to obtain a visualization of the decision borders. The resulting LDA score plot is shown in Fig. 6. The honey samples were found to be grouped clearly according to their botanical origin, with a 100% classification agreement.

VI. MODELS FOR PREDICTING THE NUTRACEUTIC INDICATORS

Partial Least Square (PLS) regression was used for predicting the concentration of sugars and potassium from Raman spectra. PLS is one of the most popular techniques for predicting quantitative variables, such as the concentration of an analyte in a multi-component mixture [45]. It is used when the predictor matrix has many collinear variables and the usual multiple linear regression cannot be applied. PLS looks for a limited number of PLS factors (PF), which are linear combinations of the original predictors. These new variables are mutually orthogonal (thus uncorrelated) and have the maximum possible covariance with the target variable, among all possible combinations of the original predictors. The idea is that each PF should be linked to a different source of data variance, with the first PF being the one most linked to the target variable.
There are two fundamental parameters for assessing the good quality of the fit:
1) Coefficient of determination, R2, which is the squared correlation coefficient between predicted and reference values for the calibration set. Thus, the closer R2 is to 1, the better the fit.
2) Root mean square error of calibration (RMSEC), and root mean square error of cross validation (RMSECV), which estimate the prediction errors on the calibration and on the validation set, respectively. The closeness of the RMSEC to the RMSECV provides an estimate of the robustness

of the predictive model. In practice, the PLS method makes it possible to predict the concentration of an analyte in an *n*th sample by means of:

$$\widehat{y_n} - \langle y \rangle = \sum_{m=1}^{M} r_m (x_{nm} - \langle x \rangle_m) \qquad (1)$$

where:
1) *M*: the number of spectral channels (discrete wavenumbers);
2) *r*m: the regression coefficient that corresponds to the *m*th wavenumber;
3) *x*nm: the value of the Raman spectrum of an *n*th sample at the *m*th wavenumber;
4) _*x*_m: the mean value of the Raman spectrum at the *m*th wavenumber, for the calibration set;
5) _*y*_: the mean value of the target variable.
The data processing was carried out by means of CAMOUnscrambler software [46]. Because of the limited number of samples available, it was not possible to divide the entire set into two sets for calibration and validation, and so the validation was carried out using the Leave-One-Out method [47]. Table III shows the parameters of the fit (R2 of calibration and validation, RMSEC and RMSECV). Indeed, the linear fit is excellent for quantifying glucose and potassium, and is good for the other analytes. Note that, although the spectra are normalized to the main peak of fructose, it is still possible to predict the fructose content. This is so because the heights of the glucose and maltose peaks are influenced by the relative abundance of all the sugars, included fructose.

VII. DETECTING UNEXPECTED TASTES

A recent trend in analytics is the correlation of sensory data to optical spectroscopy, as an ultimate attempt to replace human panels for food quality perception with a more objective instrumental evaluation. Near infrared spectroscopy has been widely used for many foodstuffs [48]–[52], and Raman spectroscopy has also provided an effective means for evaluating meat [53].
In this paper, a preliminary attempt has been made to verify whether and to what extent the Raman fingerprints of honeys can be correlated to certain tastes, especially for singling out a sample with a different taste from among similar samples. For this experiment, only chestnut honeys were considered, since one was available (named H20) that had a very different Raman spectrum compared to that of the others. This sample was intentionally discarded in the previous processing, because it heavily biased the PCA models, masking the differences between the other samples.
An electronic tongue was used to measure all the chestnut honeys, including H20. The electronic tongue was a commercially available instrument making use of seven potentiometric chemical sensors (ChemFET) with cross sensitivity to ionic, neutral and chemical compounds responsible for taste [54]. Every sensor had sensitivity to many substances, however with different detection thresholds. In practice, the sensors' cross sensitivity to citric acid, sodium chloride, glucose, caffeine and monosodium glutamate, made it possible to recognize specific food tastes, such as sour, salty, sweet, bitter and savory [55]. The radar plot of Fig. 7 illustrates the measured sensory profiles of chestnut honeys. As expected, the sample H20 showed a peculiar sensory pattern, stimulating intense responses of ZZ andHAsensors. Among the other samples, H32 and H25 caused a negligible response of HA sensor, while the others showed similar taste profiles without featuring peculiar characteristics. The outputs of all sensors were correlated to the PC1 calculated by the Raman spectra. The only nearly-linear correlation was achieved for ZZ sensor (R2 = 0.99, and RMSEC = 0.37).
Fig. 8 shows the correlation curves for ZZ and HA sensors for comparison, as they were responsible of the strange sensory pattern of H20 sample. Among all the sensors, ZZ is the most reactive to the savory-bitter taste, being mainly sensitive to caffeine and monosodium glutamate. These preliminary results
indicate that Raman spectroscopy has the potential to identify taints or unexpected tastes.

VIII. CONCLUSION

Raman spectroscopy has demonstrated good potential for the nondestructive and rapid assessment of honeys produced in the region of Calabria, above all for distinguishing their botanical origin and for predicting important nutraceutic indicators, such as the concentration of the main sugars and of potassium, and to single out unexpected tastes. Other initiatives are in progress for correlating Raman spectra to other nutraceutic indicators, such as aminoacids, proteins, enzymes, and other minerals. Moreover, the collection of honey samples will be increased in order to build a more robust and accurate model for analytics. Indeed, hand-held Raman instruments with excitation at 1064 nm are now becoming commercially available, thus making it possible to perform a wide variety of analytical measurements by means of a single spectroscopic measurement—just a light shot. This could be a cost-effective methodology with the potential of being used for fast screening during industrial process controls.

REFERENCES

[1] L. Persano Oddo, M. G. Piazza, A. G. Sabatini, and M. Accorti, "Characterization of unifloral honeys," *Apidologie*, vol. 26, pp. 453–465, 1995.
[2] L. Persano Oddo and R. Piro, "Main European unifloral honeys: Descriptive sheets," *Apidologie*, vol. 35, pp. S38–S81, 2004.
[3] [Online]. (2016). Available: http://www.apimondia.com/en
[4] M. de la Guardia and S. Garrigues, Eds., *Challenges in Green Analytical Chemistry*. Cambridge, U.K.: RSC, 2011.
[5] J. Moros, S. Garrigues, and M. de la Guardia, "Vibrational spectroscopy provides a green tool for multi-component analysis," *Trends Analytical Chem.*, vol. 29, pp. 578–591, 2010.
[6] S. Armenta, S. Garrigues, and M. de la Guardia, "Green analytical chemistry," *Trends Analytical Chem.*, vol. 27, pp. 497–511, 2008.
[7] J. Riedl, S. Esslinger, and C. Fauhl-Hassek, "Review of validation and reporting on non-targeted fingerprinting approaches for food authentication," *Analytica Chimica Acta*, vol. 885, pp. 17–32, 2015.
[8] D. I. Ellis, V. L. Brewster, W. B. Dunn, J. W. Allwood, A. P. Golovanov, and R. Goodacre, "Fingerprinting food: Current technologies for the detection of food adulteration and contamination," *Chem. Soc. Rev.*, vol. 41, pp. 5569–5868, 2012.
[9] A. M. Mouazen and A. Al-Walaan, "Glucose adulteration in Saudi honey with visible and near infrared spectroscopy," *Int. J. Food Properties*, vol. 17, pp. 2263–2274, 2014.
[10] L. Chen, J. Wang, Z. Ye, J. Zhao, X. Xue, Y. Vander Heyden, and Q. Sun, "Classification of Chinese honeys according to their floral origin by near infrared spectroscopy," *Food Chem.*, vol. 135, pp. 338–342, 2012.
[11] L. Chen, X. Xue, Z. Ye, J. Zhou, F. Chen, and J. Zhao, "Determination of Chinese honey adulterated with high fructose corn syrup by near infrared spectroscopy," *Food Chem.*, vol. 128, pp. 1110–1114, 2011.
[12] T. Woodcock, G. Downey, and C. P. O'Donnell, "Near infrared spectral fingerprinting for confirmation of claimed PDO provenance of honey," *Food Chem.*, vol. 114, pp. 742–746, 2009.
[13] K. Ruoff, W. Luginb¨uhl, S. Bogdanov, J. O. Bosset, B. Estermann, T. Ziolko, S. Kheradmandan, and R. Amad`o, "Quantitative determination of physical and chemical measurands in honey by near-infrared spectrometry," *Eur. Food Res. Technol.*, vol. 225, pp. 415–423, 2007.
[14] K. Ruoff, W. Luginb¨uhl, S. Bogdanov, J. O. Bosset, B. Estermann, T. Ziolko, S. Kheradmandan, and R. Amad`o, "Authentication of the botanical origin of honey by near-infrared spectroscopy," *J. Agricultural Food Chem.*, vol. 54, pp. 6867–6872, 2006.
[15] T. Woodcock, G. Downey, J. D. Kelly, and C. O'Donnell, "Geographical classification of honey samples by near-infrared spectroscopy: A feasibility study," *J. Agricultural Food Chem.*, vol. 55, pp. 9128–9134, 2007.

[16] G. Downey, V. Fouratier, and J. D. Kelly, “Detection of honey adulteration by addition of fructose and glucose using near infrared transflectance spectroscopy,” *J. Near Infrared Spectrosc.*, vol. 11, pp. 447–456, 2003.
[17] L. Dvash, O. Afik, S. Shafir, A. Schaffer, Y. Yeselson, A. Dag, and S. Landau, “Determination by near-infrared spectroscopy of perseitol used as a marker for the botanical origin of avocado (Persea Americana Mill.) honey,” *J. Agricultural Food Chem.*, vol. 50, pp. 5283–5287, 2002.
[18] Z. Gan, Y. Yang, J. Li, X. Wen, M. Zhu, Y. Jiang, and Y. Ni, “Using sensor and spectral analysis to classify botanic origin and determine adulteration of raw honeys,” *J. Food Eng.*, vol. 178, pp. 151–158.
[19] H. E. Tahir, Z. Xiaobo, S. Tingting, S. Jiyong, and A. A. Mariod, “Near-infrared (NIR) spectroscopy for rapid measurement of antioxidant properties and discrimination of Sudanese honeys from different botanical origin,” *Food Analytical Methods*, 2016, to be published, doi: 10.1007/s12161-016-0453-2.
[20] A. M. Gonz´alez-Param´as, R. J. Garc´ıa-Villanova, J. A. G´omez-B´arez, J. S´anchez S´anchez, and R. Ardanuy Albajar, “Botanic origin of monovarietal dark honeys (from heather, holm, oak, pyrenean oak and sweet chestnut) based on their chromatic characters and amino acid profiles,” *Eur. Food Res. Technol.*, vol. 226, pp. 87–92, 2007.
[21] J. Bong, K. M. Loomes, R. C. Schlothauer and J. M. Stephes, “Fluorescence markers in some New Zealand honeys,” *Food Chem.*, vol. 192, pp. 1006–1014, 2016.
[22] L. Lenhardt, R. Bro, I. Zekovi´c. T. Grami´canin, and M. D. Dramianin, “Fluorescence spectroscopy coupled with PARAFAC and PLS DA for characterization and classification of honey,” *Food Chem.*, vol. 175, pp. 284–291, 2015.
[23] K. Nikolova, T. Eftimov, and A. Aladjadjiyan, “Fluorescence spectroscopy as a method for quality control of honey,” *Adv. Res.*, vol. 2, pp. 95–108, 2014.
[24] R. Karoui, E. Dufour, J. O. Bosset, and J. De Baerdemaeker, “The use of front face fluorescence spectroscopy to classify the botanical origin of honey samples produced in Switzerland,” *Food Chem.*, vol. 101, pp. 314–323, 2007.
[25] K. Ruoff,W. Luginb¨uhl, R. K¨unzli, S. Bogdanov, J. O. Bosset, K. von der Ohe,W. von der Ohe, and R. Amad`o, “Authentication of the botanical and geographical origin of honey by front-face fluorescence spectroscopy,” *J. Agricultural Food Chem.*, vol. 54, pp. 6858–6866, 2006.
[26] K. Ruoff, R. Karoui, E. Dufour,W. Luginb¨uhl, J. O. Bosset, S. Bogdanov, and R. Amad`o, “Authentication of the botanical origin of honey by frontface fluorescence spectroscopy.Apreliminary study,” *J. Agricultural Food Chem.*, vol. 53, pp. 1343–1347, 2005.
[27] N. Ghosh, Y. Verma, S. K. Majumder, and P. K. Gupta, “A fluorescence spectroscopic study of honey and cane sugar syrup,” *Food Sci. Technol. Res.*, vol. 11, pp. 59–62, 2005.
[28] B. O¨ zbalci, I. H. Boyaci, A. Topcu, C. Kadılar, and U. Tamer, “Rapid analysis of sugars in honey by processing Raman spectrum using chemometric methods and artificial neural networks,” *Food Chem.*, vol. 136, pp. 1444–1452, 2013.
[29] S. Li, Y. Shan, X. Zhu, X. Zhang, and G. Ling, “Detection of honey adulteration by high fructose corn syrup and maltose syrup using Raman spectroscopy,” *J. Food Composition Anal.*, vol. 28, pp. 69–74, 2012.
[30] R. Goodacre, B. S. Radovic, and E. Anklam, “Progress toward the rapid nondestructive assessment of the floral origin of European honey using dispersive Raman spectroscopy,” *Appl. Spectrosc.*, vol. 56, pp. 521–527, 2002.
[31] J. A. Fern´andez Pierna, O. Abbas, P. Dardenne, and V. Baeten, “Discrimination of Corsican honey by FT-Raman spectroscopy and chemometrics,” *Biotechnol. Agronomical Soc. Environ.*, vol. 15, pp. 75–84, 2011.
[32] A. N. Batsoulis, N. G. Siatis, A. C. Kimbaris, E. K. Alissandrakis, C. S. Pappas, P. A. Tarantilis, P. C. Harizanis, and M. G. Polissiou, “FTRaman spectroscopic simultaneous determination of fructose and glucose in honey,” *J. Agricultural Food Chem.*, vol. 53, pp. 207–210, 2005.

[33] L. F. C. de Oliveira, R. Colombara, and H. G. M. Edwards, “Fourier transform Raman spectroscopy of honey,” *Appl. Spectrosc.*, vol. 56, pp. 306–311, 2002.
[34] M. M. Paradkar and J. Irudayaraj, “Discrimination and classification of beet and cane inverts in honey by FT-Raman spectroscopy,” *Food Chem.*, vol. 76, pp. 231–239, 2001.
[35] A. G. Mignani, L. Ciaccheri, A. A. Mencaglia, T. Verschooten, H. Ottevaere, and H. Thienpont, “Raman spectroscopy for distinguishing the composition of table-top artificial sweeteners,” *Proceedia Eng.*,vol. 87, pp. 240–243, 2014.
[36] A. G. Mignani, L. Ciaccheri, A. A. Mencaglia, R. Di Sanzo, S. Carabetta, and M. T. Russo, “Dispersive Raman spectroscopy excited at 1064nm to classify the botanic origin of honeys from Calabria and quantify the sugar profile,” *Proc. SPIE, Adv. Environ., Chem, Biol. Sens. Technol.*, vol. 9486, 2015, Art. No. 94860E.
[37] HPAEC-PAED: DIONEX ICS 3000 by Thermo Scientific [Online]. (2016). Available: http://www.thermoscientific.com/
[38] ICP-OES: Horiba JobinYvonULTIMA 2 by HORIBAScientific [Online]. (2016). Available: http://www.horiba.com/scientific/
[39] P. J. Larkin, *IR and Raman Spectroscopy: Principles and Spectral Interpretation*. Waltham MA, USA: Elsevier, 2011.
[40] BRAM-1064-HR by Bayspec, Inc. BRAM-1064-HR [Online]. (2016). San Jose CA, USA. Available: www.bayspec.com
[41] P. Missio da Silva, C. Gauche, L. V. Gonzaga, A. C. Oliveira Costa, and R. Fett, “Honey: Chemical composition, stability and authenticity,” *Food Chem.*, vol. 196, pp. 309–323, 2016.
[42] J. E. Jackson, *A User’s Guide to Principal Components*. Hoboken NJ,USA: Wiley, 2003.
[43] L. A. Berrueta, R. M. Alonso-Salces, and K.H´eberger, “Supervised pattern recognition in food analysis,” *J. Chromatography A*, vol. 1158, pp. 196–214, 2007.
[44] B. G. M. Vandeginste, D. L. Massart, L. C. M. Buydens, S. De Jong, D. J. Lewi and J. Smeyers-Verbeke, *Handbook of Chemometrics and Qualimetrics*. Amsterdam, the Netherlands: Elsevier, 1998, ch. 33.
[45] S. Wold, M. Sj¨ostr¨om, and L. Erikkson, “PLS-regression: A basic tool for chemometrics,” *Chemometrics Intell. Lab. Syst.*, vol. 58, pp. 109–130, 2001.
[46] Version 10.3 [Online]. (2016). Available: http://www.camo.com/rt/Products/Unscrambler/unscrambler.html
[47] K. H. Esbensen, *Multivariate Data Analysis—In Practice*. Oslo, Norway: CAMO AS, 2009, pp. 163–164.
[48] Q. Ouyang, Q. Chen, and J. Zhao, “Intelligent sensing sensory quality of Chinese rice wine using near infrared spectroscopy and nonlinear tools,” *Spectrochim. Acta A, Mol. Biomol. Spectrosc.*, vol. 154, pp. 42–46, 2016.
[49] J. H. Cheng and D. W. Sun, “Data fusion and hyperspectral imaging in tandem with least squares-support vector machine for prediction of sensory quality index scores of fish fillet,” *LWT-Food Sci. Technol.*, vol. 63, pp. 892–898, 2015.
[50] R. Ferrer-Gallego, J. M. Hern´andez-Hierro, J. C. Rivas-Gonzalo, and M. T. Escribano-Bail´on, “Evaluation of sensory parameters of grapes using near infrared spectroscopy,” *J. Food Eng.*, vol. 118, pp. 333–339, 2013.
[51] M. I. Gonz´alez-Mart´ın, P. Saveriano-P´erez, I. Revilla, A. M. Vivar-Quintana, J. M. Hern´andez-Hierro, C. Gonz´alez-P`erez, and I. A. Lobos-Ortega, “Prediction of sensory attributes of cheese by near-infrared spectroscopy,” *Food Chem.*, vol. 127, pp. 256–263, 2011.
[52] M. C. Ortiz, L. Sarabia, R. Garc´ıa-Rey and M. D. Luque de Castro, “Sensitivity and specificity of PLS-class modelling for five sensory characteristics of dry-cured ham using visible and near infrared spectroscopy,”
Analytica Chimica Acta, vol. 558, pp. 125–131, 2006.
[53] Q.Wang, S. M. Lonergan, and C.Yu, “Rapid determination of pork sensory quality using Raman spectroscopy,” *Meat Sci.*, vol. 91, pp. 232–239, 2012.

[54] E-Tongue ASTREE by AlphaMOS [Online]. (2016). Available: http://www.alpha-mos.com/analytical-instruments/astree-electronictongue.
[55] Z. Wei, J. Wang, and W. Liao, “Technique potential for classification of honey by electronic tongue,” *J. Food Eng.*, vol. 94, pp. 260–266, 2009.

TABLE I
THE COLLECTION OF HONEYS ANALYZED

ID Code	Botanical origin	Geographical area
TC	Chestnut	Aspromonte mountains
H25		Aspromonte mountains
H28		Mongiana (VV), 900 m
H32		Gimigliano (CZ), 600 m
H30		Savini Serre, Aspromonte, 700 m
TA	Citrus	Rosarno, Gioia Tauro (RC)
H14		San Vito sullo Ionio (CZ)
H19		Catona (RC)
H23		Rosarno, Gioia Tauro (RC)
H27		Pizzo (VV)
H21	Acacia	Lagamadi (RC)
H26		Filogaso (VV)
H31		Tropea (VV), 700 m

TABLE II
MAIN SUGARS OF HONEYS AND THEIR RAMAN BANDS

Band (cm^{-1})	Main contribution	Secondary contribution
707	Fructose	
821	Fructose	
867	Fructose	Glucose
917	Glucose	Maltose
1060–1080	Fructose	Glucose
1127	Glucose	Maltose
1267	Fructose	Glucose
1372	Glucose	Maltose
1460	Fructose	Glucose

TABLE III
PARAMETERS OF THE FIT FOR MULTI-COMPONENT ANALYSIS

Analyte		RMSEC	R^2 (cal)	RMSECV	R^2 (val)
Sugars (mg/g)	Glucose	7.3	0.96	11	0.92
	Fructose	5.5	0.89	7.6	0.82
	Maltose	3.5	0.83	5.3	0.66
	DS-TIKN	2.3	0.91	3.6	0.83
	Total TS	2.6	0.89	3.9	0.80
Potassium (μg/g)		0.3	0.97	0.5	0.94

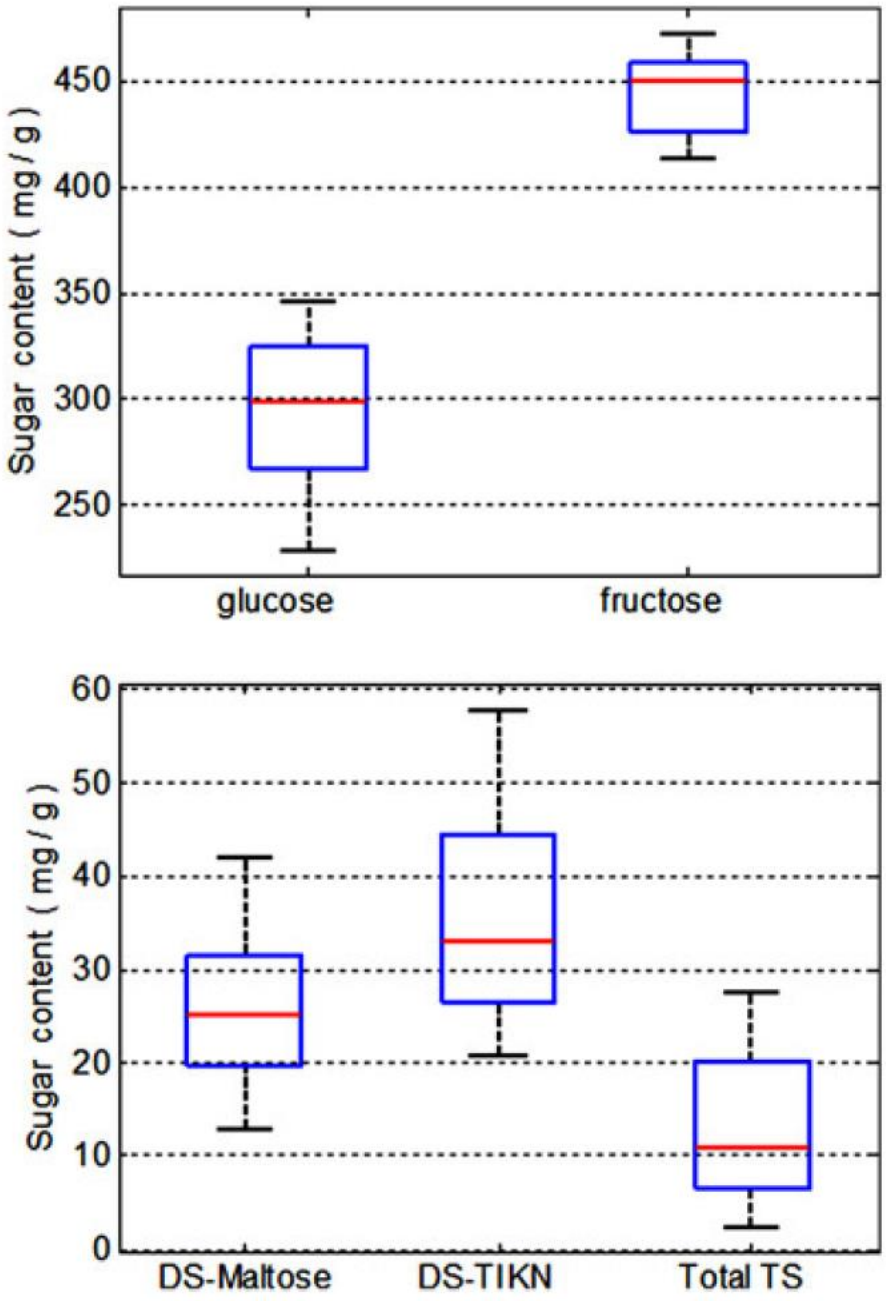

Fig. 1. Boxplots of sugar concentrations: glucose and fructose (upper plot); maltose, other di-saccharises, and tri-saccharides (lower plot).

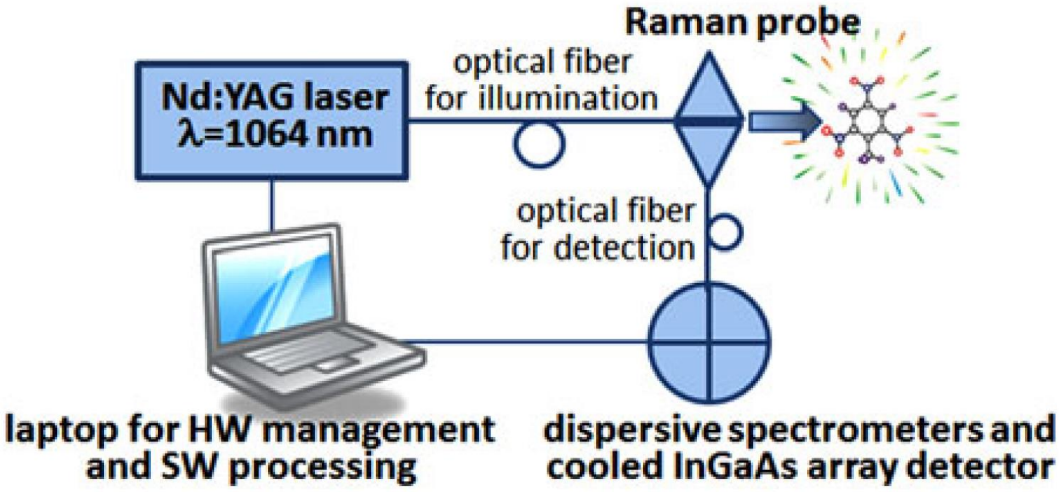

Fig. 2. Working principle of the Raman spectroscopy setup.

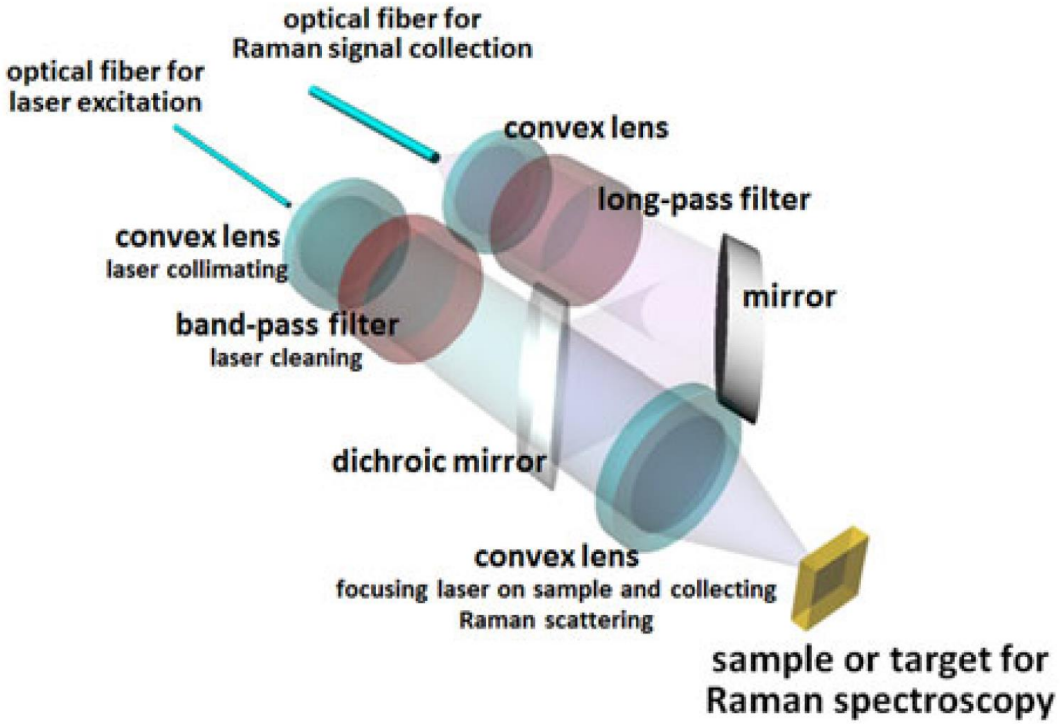

Fig. 3. Diagram of the microoptic unit for illumination and detection.

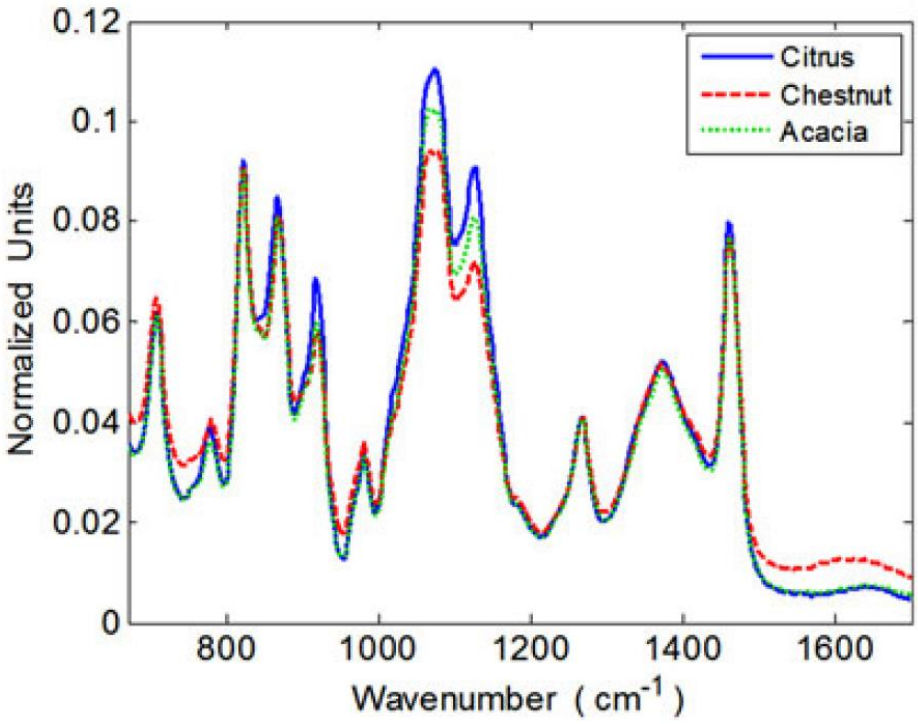

Fig. 4. Raman spectra of honeys averaged according to the botanical origin.

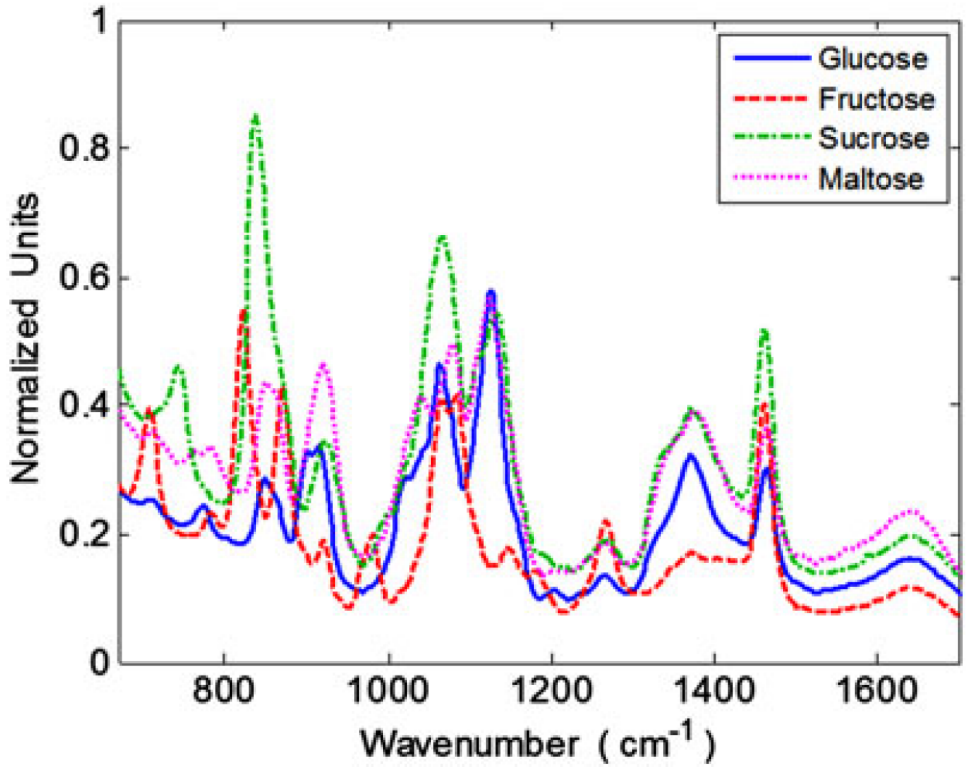

Fig. 5. Raman spectra of water solutions (30% w/w) of the main sugars.

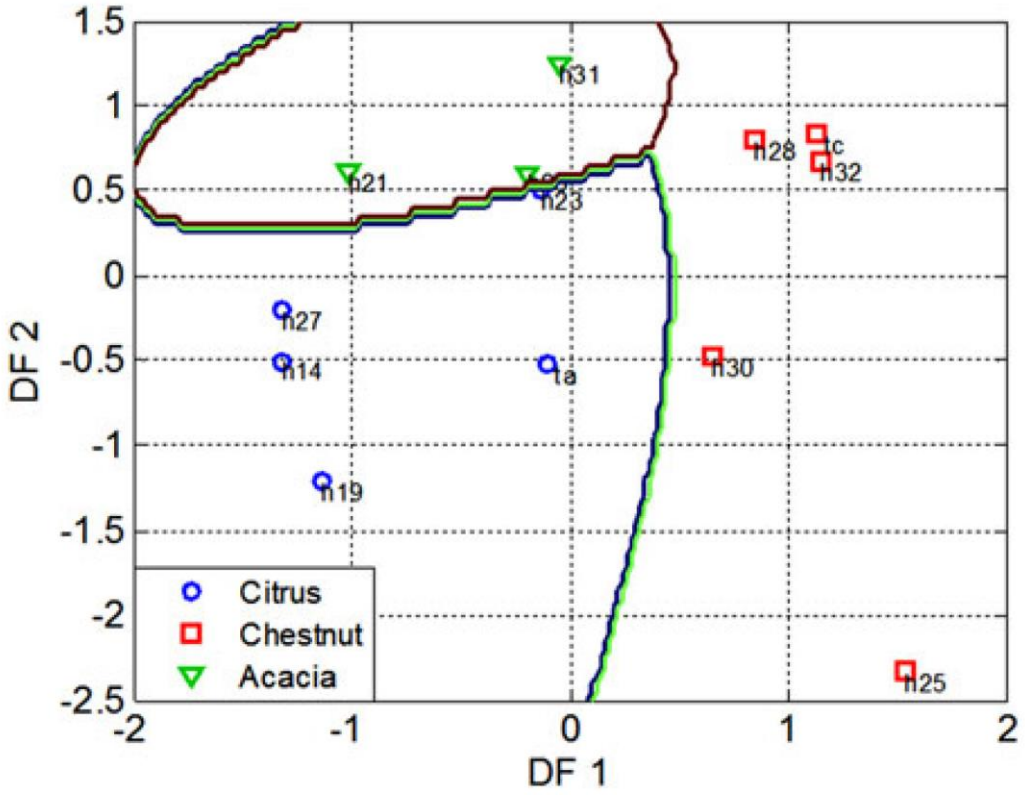

Fig. 6. Results of LDA processing of PC1 and PC2 scores, which cluster the samples according to the botanical origin with 100% classification agreement.

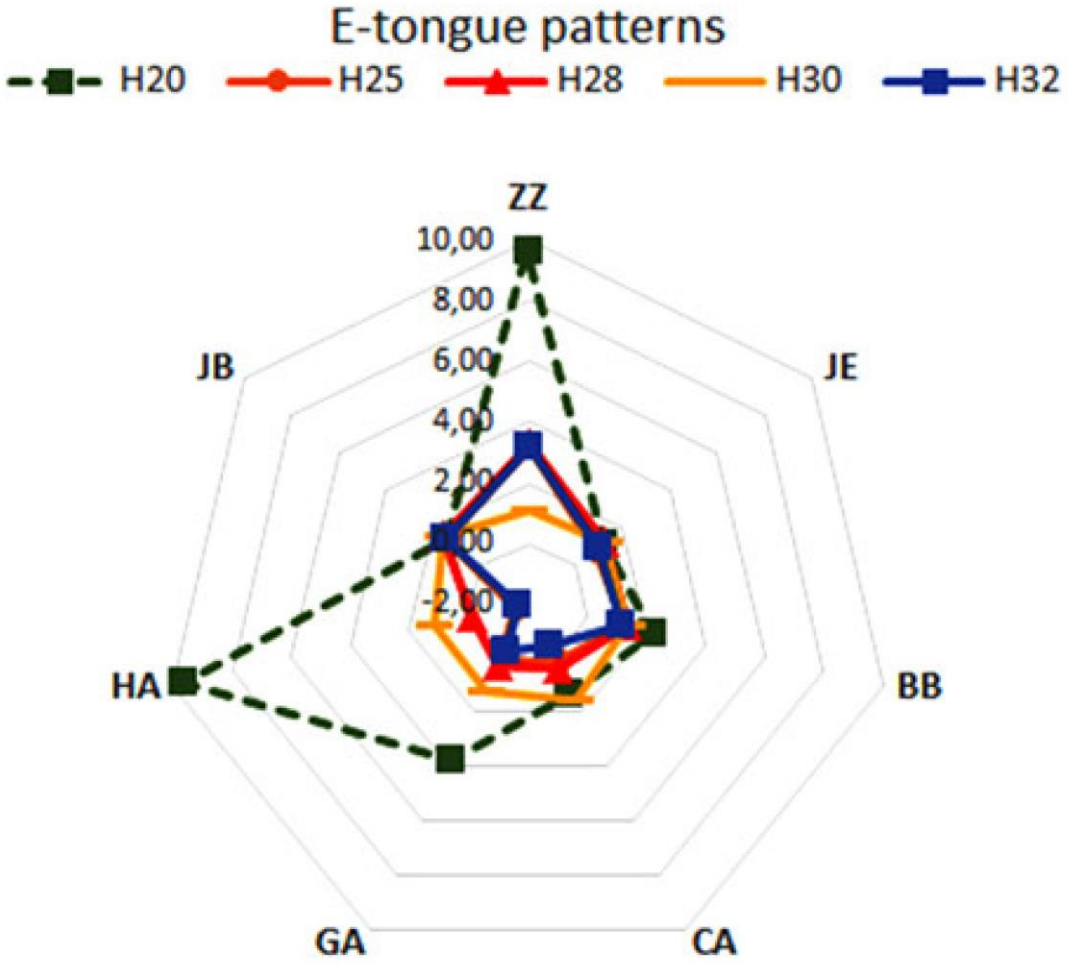

Fig. 7. Sensory profiles of chestnut honeys measured by electronic tongue.

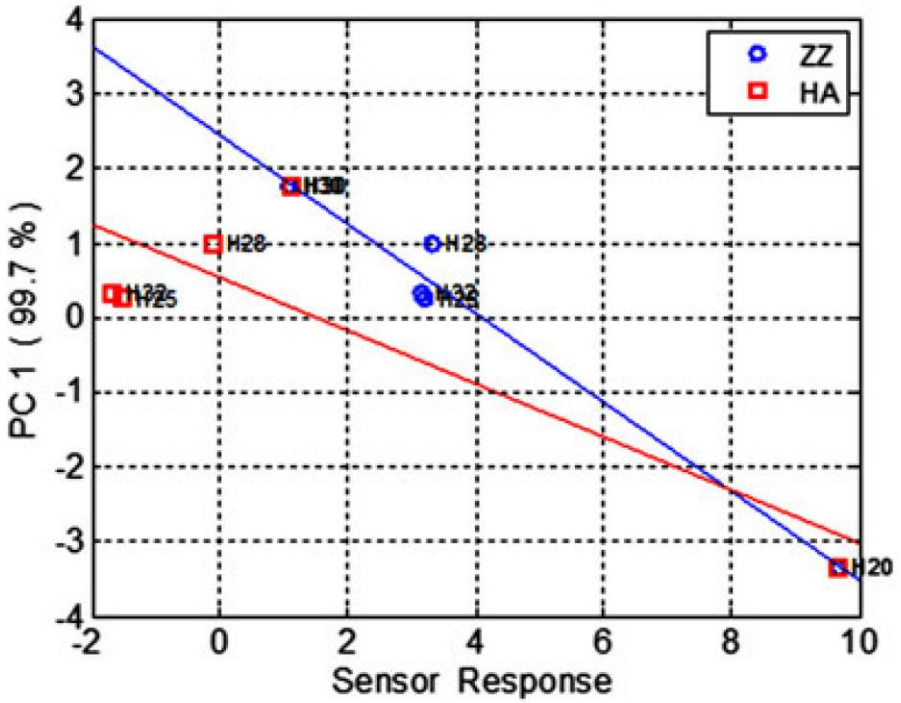

Fig. 8. Correlation of ZZ and HA sensor outputs with Raman spectra of chestnut honeys.